Exciton spin polarization in magnetic semiconductor quantum wires

O. Ray, A. A. Sirenko, J. J. Berry, and N. Samarth[a)]
Department of Physics, Pennsylvania State University, University Park, Pennsylvania 16802

J. A. Gupta, I. Malajovich, and D. D. Awschalom
Department of Physics, University of California, Santa Barbara, Santa Barbara, California 93106

(Received 12 November 1999; accepted for publication 3 January 2000)

Electron-beam lithography and wet etching techniques are used to laterally pattern ZnSe/(Zn,Cd,Mn)Se single quantum wells into magnetically active quantum wires with widths ranging from 20 to 80 nm. Photoluminescence spectroscopy as a function of wire width reveals a competition between elastic strain relaxation and quantum confinement. Magnetophotoluminescence measurements at low temperatures indicate a strong exciton spin polarization due to the *sp–d* exchange-enhanced spin splitting, ranging from 20% to 60% at 4 T. © *2000 American Institute of Physics.* [S0003-6951(00)01409-1]

Nanopatterned semiconductor structures such as quantum wires (QWRs) and quantum dots (QDs) have generated substantial interest over the past decade, motivated primarily by the effects of reduced dimensionality on the electronic density of states (DOS).[1] Recently, there is growing interest in magnetic semiconductor (MS) nanostructures where the reduced dimensionality and the modified density of states influence the interplay between electronic and magnetic phenomena.[2] The controlled fabrication and fundamental understanding of such nanostructures is crucial to the development of semiconductor-based ''spintronic'' devices[3] and spin-based quantum computation schemes[4] that rely on the transfer of spin information between the nanostructured components. Although progress has been made in the understanding of MS quantum wells, studies of MS QDs (Ref. 5) and QWRs (Ref. 6) are still at a nascent stage. In this work, we exploit patterning procedures developed earlier[7,8] for nonmagnetic (Zn,Cd)Se-based nanostructures to yield one-dimensional (1D) MS QWRs with widths as small as 20 nm without degradation of the magneto-optical properties.

A series of QWRs of varying width are patterned from a $ZnSe/Zn_{1-x-y}Cd_xMn_ySe$ heterostructure grown by molecular-beam epitaxy on a (100) GaAs substrate, following the deposition of a 800 nm ZnSe buffer layer. Quantum confinement in the growth direction (z) is created by using an entirely ''digital'' scheme[9] in which coherently strained CdSe monolayers and MnSe submonolayers are interspersed within a ZnSe matrix. This digital alloy region consists of four periods of a short period superlattice of $(ZnSe)_{m-f-g}(MnSe)_f(CdSe)_g$ ($m=5$ ML, $f=1/8$ ML, and $g=1$ ML) followed by 1 ML of CdSe and finished with a 15 nm ZnSe cap layer. This region acts as a single quantum well (SQW) of ~6 nm width. All growth rates are determined using *in situ* reflection high-energy electron diffraction. For the patterning process, the samples are spin coated with nominally 100-nm-thick electron-beam resist poly(methylmethacrylate) (PMMA) of molecular weight of 950 K. The patterns are defined on the sample using direct-write electron-beam lithography at an electron energy of 50 keV. Multiple wire fields of 100×100 μm^2 area are defined on each sample, with the wire width varying from 30 to 150 nm between the different fields. A 13 nm Ti layer is evaporated following development in MIBK:IPA (1:3). Ti wires, which serve as hard masks for the subsequent wet etch, are obtained using lift-off and the pattern is then transferred into the semiconductor by wet etching to a depth of 60–70 nm with a solution of $K_2Cr_2O_7$:HBr:H_2O (1:130:250) at room temperature. Using scanning electron microscopy (SEM) and atomic-force microscopy (AFM), we estimate that the wire widths range from 20 to 80 nm at the quantum well. In order to minimize tip effects in the tapping-mode AFM images of these high aspect ratio (1:4) structures, high-resolution silicon tips with a nominal full tip angle of 20° are employed. Tilted-view SEM images of QWRs before removal of the Ti mask (Fig. 1) show a significant undercutting of nearly 50% postetching, resulting in wires much narrower than the Ti mask widths. We note that due to the anisotropic nature of the etch employed, the QWRs need to be aligned along the (011) axis in order to obtain nearly vertical and steep sidewalls postetching.

Low-temperature photoluminescence (PL) measurements are performed using either 410 nm excitation from a frequency-doubled Ti–sapphire laser or 325 nm excitation from a He–Cd laser focused to a 75-μm-diam spot, with excitation densities ranging from 10 to 70 W/cm^2. Magneto-PL is measured in an optical cryostat with a split-coil 7 T magnet in the Faraday geometry. The zero-field PL from the magnetic QWRs is similar to that reported for

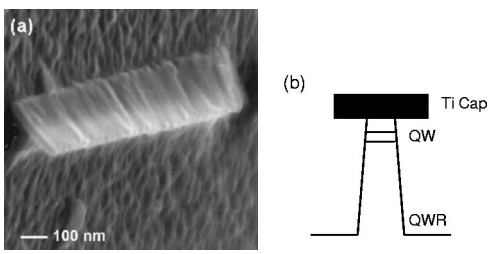

FIG. 1. (a) SEM image of a 75-nm-wide wire with the Ti mask (150 nm) present. A high degree of undercutting (~50%) is visible. (b) Schematic of an etched QWR with the Ti cap present.

a)Electronic mail: nsamarth@psu.edu

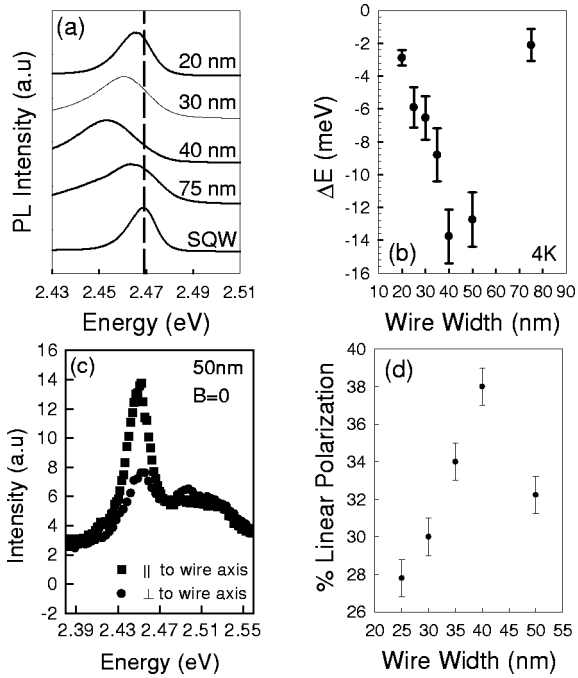

FIG. 2. (a) PL spectra at 4 K from wires of different widths. (b) Shift of PL peak position (at 4 K) for different wire widths. The shift is with respect to the PL peak from the SQW. (c) Linear polarization of PL from 50 nm QWRs. (d) Variation of degree of linear polarization with QWR width.

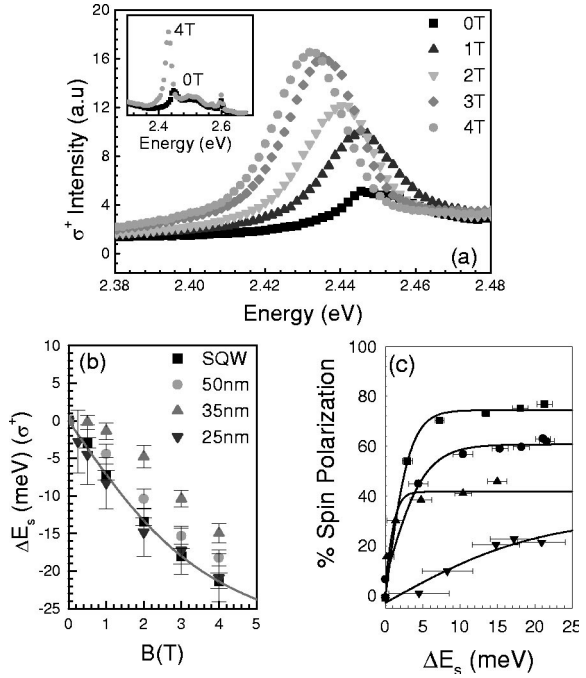

FIG. 3. (a) Magnetic-field dependence of the circular polarization-resolved (PL) (σ^+) from 35 nm QWRs at 4 K. The inset shows the magnetic-field variation over a wider spectral range. (b) Zeeman shift of the σ^+ PL peak for all QWR samples, and the SQW, at 4 K. The solid line shows a modified Brillouin function fit to the SQW data, with a saturation Zeeman shift of 32 meV and an effective temperature of $T+T_0=8$ K. (c) Variation of exciton spin polarization with Zeeman shift for the samples shown in (b). Solid lines show fits to a two-level model.

(Zn,Cd)Se QWRs:[10] the principal peak in the PL spectrum has a full width at half maximum in the range 25–35 meV for varying wire sizes and is centered at a lower energy with respect to the heavy-hole (hh) excitonic PL from a SQW (patterned mesa on the sample) [Figs. 2(a) and 2(b)]. The nonmonotonic dependence of the redshift on QWR width [Fig. 2(b)] is consistent with competition between the blueshift created by a weak lateral quantum confinement and a redshift due to partial strain relaxation at the sidewalls, the latter being dominant for the larger wires. As the exciton Bohr diameter in the confining region is estimated at ~6 nm, substantially narrower wires would be required to observe strong quantum confinement effects. Processing also creates additional PL peaks observable at low-excitation intensities; as shown later, magneto-optical spectroscopy helps identify these as defect related and not intrinsic QWR luminescence.

The PL shows a marked linear polarization parallel to the QWR axis [Figs. 2(c) and 2(d)]. In Fig. 2(d), the degree of linear polarization is defined as $(I_{\parallel}-I_{\perp})/(I_{\parallel}+I_{\perp})$, where $I_{\parallel}$ and $I_{\perp}$ are the PL intensities for linear polarization parallel and perpendicular to the wires, respectively. No polarization anisotropy is observed for the SQW. The correlation between linear polarization and the PL redshift [Figs. 2(b) and 2(d)] suggests that strain relaxation may be responsible for the observed polarization anisotropy. The compressive biaxial strain in the active region of the QWRs removes the degeneracy between hh and light-hole (lh) states. Hence, strained QWRs are not expected to show substantial linear polarization anisotropy. However, relaxation of this strain would lead to a higher degree of hh–lh mixing, and consequently, to polarization anisotropy. This is consistent with the observation that the maximum polarization anisotropy is present for wires with the largest PL redshift. In the narrowest QWRs, the onset of in-plane quantum confinement provides a competing mechanism that removes the lh–hh mixing, thus reducing the polarization anisotropy.

The application of a magnetic field reveals the magnetic nature of the QWRs through an enhancement of the Zeeman shifts. An applied magnetic field splits the hh exciton into lower- (spin-down, $J_Z=+1$) and higher-energy (spin-up, $J_Z=-1$) states, with the spin-splitting ΔE enhanced by the *sp–d* exchange between excitons and Mn^{2+} ions.[2] With increasing field, the PL is dominated by the radiative decay of lower-energy spin-down hh excitons and hence, shows a redshift, becoming strongly circularly polarized in the process. The situation may be expected to be more complex in the QWRs because of lh–hh mixing. Nonetheless, the spin-polarization-resolved magneto-PL in QWRs displays a large redshift [Figs. 3(a) and 3(b)] as well as a significant exciton spin polarization [Fig. 3(c)], indicating that the hh contributions to the confined exciton states are dominant in the PL. The spin polarization in Fig. 3(c) is defined as $(I^+-I^-)/(I^++I^-)$, where I^+ and I^- are the *peak* intensities corresponding to oppositely circularly polarized emission from spin-down and spin-up excitons, respectively. The magneto-PL distinguishes the intrinsic QWR luminescence from extrinsic defect features in the PL which do not show large Zeeman shifts [inset to Fig. 3(a)]. We also note that the magnetic-field-induced increase in PL intensity [Fig. 3(a)] is a commonly observed (but not well-understood) feature in many MS quantum structures,[9] and not unique to these QWRs.

Since the Zeeman shift (ΔE_s) of the PL is expected to follow the sample magnetization,[2] we model the shift as $\Delta E_s=(\Delta E)_{\mathrm{sat}}B_{5/2}[(5\mu_B B)/k(T+T_0)]$, where $B_S(x)$ is a

modified Brillouin function for $S=5/2$ in which the parameter T_0 accounts for $Mn^{2+}-Mn^{2+}$ interactions.[2] A comparison between magneto-PL measurements on the SQW and the QWRs [Fig. 3(b)] indicates that within the error bars set by the PL linewidths, neither the saturation value of the Zeeman shift $(\Delta E)_{\text{sat}}$ nor the parameter T_0 changes between the various wires, showing that nanopatterning does not alter the sample magnetization nor the strength of the *sp–d* and *d–d* exchange interactions. In contrast, systematic changes are observed in the exciton spin polarization as the QWRs are made narrower [Fig. 3(c)]. Regarding the spin-down and spin-up exciton states as a two-level system with an energy difference $\Delta E=2\Delta E_s$, the exciton spin polarization is fit to a thermal distribution given by $\tanh(\Delta E_S/kT)$ [solid lines in Fig. 3(c)]. The effective temperatures in these fits are 37, 60, 17, and 241 K for the SQW, 50 nm QWR, 35 nm QWR, and 25 nm QWR, respectively. These fits imply that the spin-polarized excitons do not equilibrate thermally. Furthermore, Fig. 3(c) shows that, at a given value of exciton splitting, the spin polarization decreases with QWR width, suggesting a possible increase in spin-flip scattering between the spin-up and spin-down states as the lateral dimensions are reduced.

In conclusion, we have used electron-beam lithography and wet etching to fabricate magnetic semiconductor QWRs with widths as small as 20 nm. PL measurements in zero-magnetic field indicate that the ground-state energy of the electronic states is determined by a competition between partial strain relaxation and a weak lateral quantum confinement. Further, magneto-PL studies demonstrate that nanopatterning down to ~20 nm preserves the *sp–d* exchange-enhanced spin splitting and large exciton spin polarization characteristics of two-dimensional and three-dimensional magnetic semiconductor systems. These ''spin'' QWRs provide promising templates for future studies of spin-polarized transport and spin dynamics of excitons and free carriers in 1D systems.

This work is supported by Grant Nos. ARO-DAAG55-98-1-0366, ONR N00014-99-1-0077 and -0071, DARPA/ONR N00014-99-1-1096 and -1093, and NSF DMR 97-01072 and -01484. J.J.B. and I.M. acknowledge fellowship support from the National Science Foundation.

[1] *Optical Spectroscopy of Low Dimensional Semiconductors*, edited by G. Abstreiter, A. Aydlini, and J. P. LeBurton, NATO ASI Series (Kluwer Academic, The Netherlands, 1997).
[2] D. D. Awschalom and N. Samarth, J. Magn. Magn. Mater. **200**, 130 (1999).
[3] G. Prinz, Science **282**, 1660 (1998).
[4] A. Imamoglu, D. D. Awschalom, G. Burkard, D. P. DiVincenzo, D. Loss, M. Sherwin, and A. Small, Phys. Rev. Lett. **83**, 4204 (1999).
[5] P. A. Crowell, V. Nikitin, J. A. Gupta, D. D. Awschalom, F. Flack, and N. Samarth, Physica E (Amsterdam) **2**, 854 (1998).
[6] J. Jaroszyński, G. Karczewski, J. Wrobel, T. Andrearczyk, A. Strycharczuk, T. Wojtowicz, G. Grabecki, E. Papis, E. Kamińska, A. Piotrowska, and T. Dietl, Physica E (Amsterdam) (in press).
[7] R. Steffen, Th. Koch, J. Oshinowo, F. Faller, and A. Forchel, Appl. Phys. Lett. **68**, 223 (1996).
[8] M. Illing, G. Bacher, T. Kummell, A. Forchel, T. G. Anderson, D. Hommel, B. Jobst, and G. Landwehr, Appl. Phys. Lett. **67**, 124 (1995).
[9] S. A. Crooker, D. A. Tulchinsky, J. Levy, D. D. Awschalom, R. Garcia, and N. Samarth, Phys. Rev. Lett. **75**, 505 (1995).
[10] T. Kummell, G. Bacher, A. Forchel, G. Lermann, W. Kiefer, B. Jobst, D. Hommel, and G. Landwehr, Phys. Rev. B **57**, 15439 (1998); Y. M. Niquet, C. Priester, and H. Mariette, *ibid.* **55**, R7387 (1997).